Applied Surface Science 404 (2017) 238–245

Contents lists available at ScienceDirect

Applied Surface Science

journal homepage: www.elsevier.com/locate/apsusc

Full Length Article

Vertical few-layer graphene/metalized Si-nanocone arrays as 3D electrodes for solid-state supercapacitors with large areal capacitance and superior rate capability

Baogang Quan[a], Yuena Meng[b], Lin Li[a], Zehan Yao[a], Zhe Liu[a], Kai Wang[c], Zhixiang Wei[b], Changzhi Gu[a,*], Junjie Li[a,*]

[a] Beijing National Laboratory for Condensed Matter Physics, Institute of Physics, Chinese Academy of Sciences, Beijing, 100190, China
[b] National Center for Nanoscience and Technology, 100190, China
[c] Institute of Electrical Engineering, Chinese Academy of Sciences, Beijing, 100190, China

ARTICLE INFO

Article history:
Received 18 November 2016
Received in revised form 24 January 2017
Accepted 31 January 2017
Available online 1 February 2017

Keywords:
Few-layer Graphene
Metalized Si-nanocone arrays
3D electrodes
Solid-state supercapacitors
Superior rate capability
Large areal capacitance

ABSTRACT

A strategy to promote the energy density of graphene-based supercapacitors by a combination of dry etching and chemical vapor deposition (CVD) techniques is demonstrated. A three dimensional (3D) electrode is composed of vertically oriented graphene that is deposited on metalized silicon nanocones. The design of the 3D electrodes improves specific surface area, electrolyte ion migration and electrical contact, resulting in an enhancement of areal capacitance and rate capability. Furthermore, a solid-state supercapacitor was prepared based on the 3D graphene electrodes and gel polymer electrolyte. The 3D electrode with 10 min of CVD growth of graphene endows the electrical double layer capacitor with the highest areal capacitance of 667.2 $\mu F\,cm^{-2}$, which is larger than that of supercapacitors with flat electrodes.

1. Introduction

Supercapacitors have become one of the most promising energy storage systems for renewable energy applications due to advantages over batteries in power density, cycling stability and cycle-life [1–3]. However, a major shortcoming of supercapacitors is that the energy density, which depends on the electrode capacitance and the cell voltage, is at least one order of magnitude lower than that of batteries, so it needs to be promoted for practical applications. The trend of supercapacitor research and development is improving the energy storage capability of the supercapacitors without sacrificing their power density and cycle life [4]. Generally, the performance of supercapacitors is mainly determined by the electrode materials. Recently, a great deal of research effort has been made to promote the performance of supercapacitors by exploiting nanostructured electrode materials [5–7]. However, the performance of experimentally obtained supercapacitors of carbon-based electrodes remains lower than expected, at given specific surface area value.

Graphene-based materials are promising candidates for electrical double layer capacitors (EDLCs) due to their extraordinary intrinsic properties [8,9] such as high conductivity, exceptional chemical stability and extremely high specific surface area value [10]. Up to now, several effective and convenient approaches, including chemical or thermal reduction of graphene oxide, organic solvent exfoliation of graphite, chemical vapor deposition (CVD), have been developed to synthesize graphene-based materials as electrode materials. Chemical reduction of graphene oxide is most widely used process in chemistry labs to create active materials for supercapacitors [11–13]. However, this method brings a lot of defects such as pores, oxygen functional groups and impurities on the surface of the graphene layer, which limits its electrochemical performance [14]. Besides, there is strong π-π interaction between graphene layers, which makes graphene layers tend to aggregate with each other. That aggregation greatly reduces the active area of graphene, affecting its electrochemical performance [15,16]. Therefore, it is very important to develop a way to produce graphene with high quality while keeping a large surface area at the same time [17].

Graphene grown by CVD [1,18,19] is a class of graphene with the characteristics of higher chemical purity and higher quality when compared with reduced graphene oxide [20,21]. Thus, no side electrochemical reactions are introduced during the electri-

* Corresponding authors.
E-mail addresses: czgu@iphy.ac.cn (C. Gu), jjli@iphy.ac.cn (J. Li).

http://dx.doi.org/10.1016/j.apsusc.2017.01.312
0169-4332/

cal double layer charge/discharge process, which leads to a high response rate and high power density [22]. Moreover, the graphene directly grown on the current collector possesses excellent contact between electrode materials and current, which reduces the contact resistance. However, the drawback of CVD grown two-dimensional graphene for EDLCs is that it can produce only a few layers, which cannot provide high capacitance per unit area. To obtain large capacitance per unit area (Areal capacitance) is quite important for real applications, especially for integrated circuits or on-chip device systems [23]. Although thicker graphene layer can be obtained by prolonging the growth time, it brings a restacking of graphene layers and hinders the ion diffusion, which reduces the capacitance and rate capability of the supercapacitors. But vertically oriented graphene with three-dimensional (3D) configuration of graphene nanosheets can provide channels for electrolyte ions to migrate freely between electrodes and hence further reduce the ion diffusion resistance, which is highly desirable for graphene-based supercapacitor electrodes [24]. Ren et al. used Ni foam substrate to further enhance the specific capacitance without reducing the power level [12]. Qi et al. develop an 3D vertically oriented graphene -nanocup hybrid structure for high-performance supercapacitors [25]. Yang et al. discuss the edge effect in vertically oriented graphene supercapacitor [26]. Since the perpendicular grown graphene nanosheets provide a numerous efficient transport pathway for the electrolyte ions, vertically oriented graphene can minimize electronic and ionic resistances and provide a high power level and an outstanding rate performance. However, due to the flexibility of graphene, preparation of vertically oriented graphene layers with film thickness in microns is very difficult.

In order to address this issue, we propose an approach that combines silicon nanocone with vertically oriented few-layer graphene, which is directly deposited on metalized Si nanocone arrays, to obtain 3D graphene-based electrodes. Furthermore, this well-defined 3D graphene electrode is assembled to solid-state graphene supercapacitor that shows large areal capacitance, superior rate capability and cyclic stability. This novel electrode structure with 3D nanostructured current collector and vertically oriented graphene (Fig. 1a) can promote the main characteristics of supercapacitors: energy density (i.e. capacitance) and power density (i.e. rate capability). The excellent performance is ascribed the unique structure of the electrode. First, the silicon nanocone arrays can efficiently enhance the surface area by a factor of ca. 6, which improves the loading amount of active materials per unit area on the Si chip. Second, the graphene that is directly deposited on the current collectors by CVD possesses outstanding electric contact, which reduces the contact resistance between the graphene and the current collectors and enhances the adhesion of the graphene with the current collectors [13]. In addition, the open structure among the silicon nanocones, together with the vertical orientation, benefits the ion diffusion during the charge/discharge process and results in an improved rate capability. All these factors endow the EDLCs an area specific capacitance of 667.2 $\mu F\,cm^{-2}$, which is several times than the supercapacitor with vertically aligned graphene on a flat electrode, as well as good rate capability and stable cycle life.

2. Experimental section

2.1. Preparation of silicon nanocones

The silicon nanocone array was firstly fabricated on the clean silicon substrate with highly doped n type silicon wafer using a low temperature etching process in an inductively coupled plasma (ICP) etching system (Plasmalab system 100, Oxford instruments). The detailed procedure for fabricating the silicon nanocone array was as follows: first a cleaned silicon substrate was etched by a self-mask process in an ICP system to form the nanocone structure, using SF_6 (50 sccm) as the etching gas and O_2 (10 sccm) as the passivation gas.

2.2. Growth and characterization of vertically oriented graphene

The vertically oriented graphene was uniformly grown with respect to the silicon nanocone surfaces in a CVD system (DC450, China) using Ar, H_2 and CH_4 mixture (45:1:5 sccm) gas as source. In order to lower the contact resistance between the graphene and the current collector, a 200 nm thick Ni film was deposited directly on the silicon nanocone array by a magnetron sputtering system (FJLX500, China) before HFCVD growth of the vertically oriented graphene. Samples characterization, including SEM, HRTEM and Raman spectra, were conducted by a field-emission scanning electron microscope (Hitachi S4800, Japan), a transmission electron microscope (Tecnai F20 Super-Twin, FEI, USA) and a Raman spectrometer (JY T-64000, France). The Raman spectrum measurements were completed with the excitation laser wavelength of 532 nm and the power of 0.65 mW. Both SEM images and Raman spectra of graphene were obtained from as grown graphene samples. For HRTEM images of graphene, the sample had to be scraped and transferred to TEM grids.

2.3. Fabrication of vertically oriented graphene-based EDLC devices

Silicon nanocone array-Ni-graphene samples were used directly as electrodes for supercapacitors. Two 3D graphene electrode plates with similar active areas were placed face-to-face and adhered by poly(vinyl alcohol)-KOH (PVA-KOH) polymer-gel electrolyte. The polymer-gel electrolyte was prepared by mixing 1 g of KOH and 1 g of PVA (M_w = 85,000–124,000, Sigma Aldrich) into 10 ml deionized water and heated up to 80 °C under stirring for 2 h. A 0.2 ml of PVA-KOH polymer-gel electrolyte was drop-cast onto one of the electrodes and then covered with another chip and solidified overnight to form an all-solid sandwich supercapacitor. The polymer gel electrolyte serves as both electrolyte and separator for the 3D vertically oriented graphene-based EDLCs. Conductive silver adhesive was then pasted on the end of the active area of the electrode to connect the device in the circuit.

2.4. Electrochemical characterization

All electrochemical studies of EDLCs were performed on a VMP3 potentiostat (Princeton Applied Research, USA) in a two-electrode setup at room temperature. The performance of the supercapacitor cells was analyzed using cyclic voltammetry (CV) and electrical impedance spectroscopy (EIS) to evaluate the specific capacitance, resistance and stability. CV tests were performed at scan rates of 50–10,000 mVs^{-1} with a potential ranging from 0 to 1 V. EIS measurements were performed at open circuit voltage by applying a sinusoidal signal of 10 mV amplitude at frequencies ranging from 100 kHz to 1 Hz. The capacitance values were calculated by integrating over the full CV curve to determine the average values, and specific capacitances were calculated based on the area of the device stack.

3. Result and discussion

3.1. Characterization of 3D graphene electrodes

Our fabrication route for the implementation of our proposed design is a convenient and cost-effective process. Fig. 1a shows a

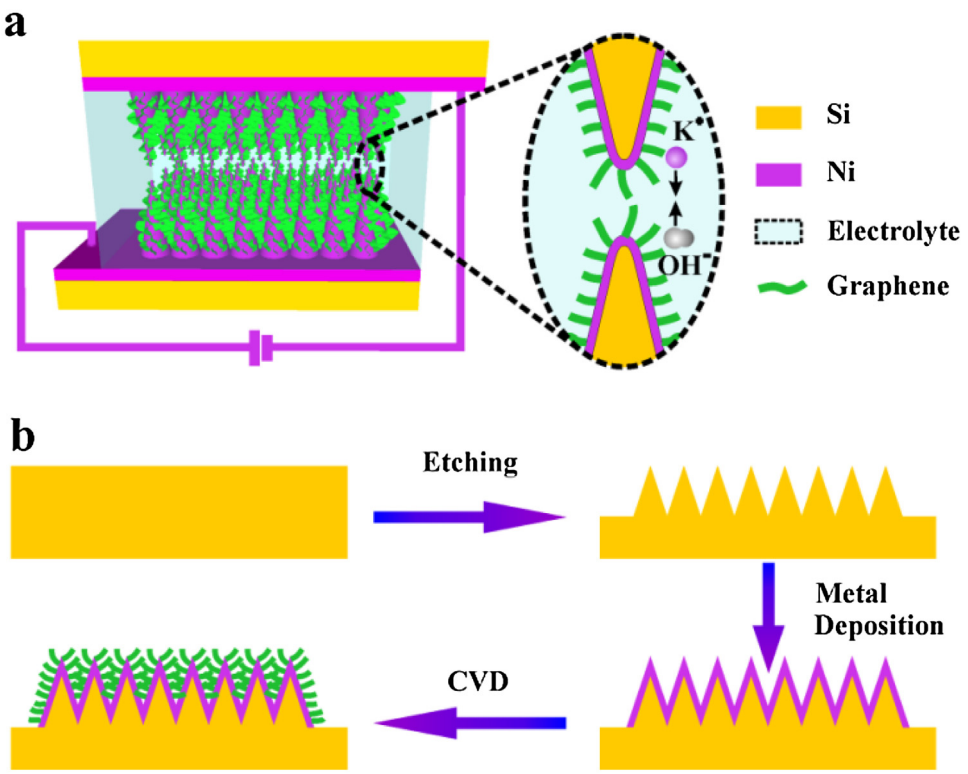

Fig. 1. (a) Schematic of the structure of EDLCs based on electrodes with a 3D nanostructured current collector and vertically oriented graphene and (b) schematic of the fabrication process of 3D graphene-based electrodes.

schematic of the structure of EDLCs based on electrodes with a 3D nanostructured current collector and vertically oriented graphene. Fig. 1b presents the schematic diagram of the fabrication process of 3D graphene electrodes from a highly doped silicon wafer to graphene nanosheets grown on silicon nanocone arrays by using ICP self-masked etching and later CVD growth process. The morphology of the as fabricated silicon nanocone arrays were characterized by scanning electron microscopy (SEM), as shown in Fig. 2a. The average height of the silicon cones is approximately 900 nm, with tip radii below 10 nm, and their areal distribution density is about $\sim 1 \times 10^9$ cm^{-2}. The fabrication of silicon nanocones is an efficient solution to enlarge the surface area of the silicon current collector substrate. The silicon nanocone arrays were used as the current collector after growth of vertically aligned graphene to act as electrodes for EDLCs. However, the Nyquist plot of Si nanocone-graphene electrode (see Fig. S1, Supplemental information) obtained by electrical impedance spectroscopy (EIS) reveals that there is a large equivalent series resistance, which has a negative effect on electron transferring in an EDLC. In order to lower the internal resistance of the supercapacitor, Ni thin film was deposited with a thickness of 200 nm by magnetron sputtering method. After this procedure, vertically oriented graphene was grown on the surface of the silicon nanocones by chemical vapor deposition (CVD) [27]. Finally, vertically oriented graphene deposited on the Ni film-covered Si nanocone array was used directly as 3D electrodes for supercapacitors.

The graphene nanosheets completely cover the surface of Si nanocone arrays, as presented by the SEM image of Fig. 2b. The high-resolution SEM image gives a clear view of graphene-based electrodes, and all graphene sheets are vertically oriented with respect to the surface of the cones (Fig. 2c). So the vertically oriented graphene on 3D electrode has an edge-on feature, which is favorable for use in EDLCs. Each sheet of this vertically oriented graphene is physically isolated from the others and leaves a space with flare angle between graphene sheets as a result of the CVD growth mechanism [27]. Compared with vertical graphene nanosheets grown on the flat substrate of silicon wafer, as shown in Fig. 2d, graphene on Si nanocone arrays greatly enhance the surface area, which is favorable for the required electrochemical properties. The vertically oriented graphene based electrodes with growth-time of 10 min were dubbed VOG-10. Fig. 2e is a transmission electron microscopy (TEM) image of few-layer graphene scraped from a vertically oriented graphene sample, revealing a very thin sheet structure of graphene. The edges of graphene nanosheet are shown in a TEM image (Fig. 2e), which distinctly presents the sharp edge with few layers. Fig. 2f is a high resolution TEM image clearly revealing the details of the few-layer graphene nanosheet. It can be observed from Fig. 2g that a large number of graphene layers have exposed edges, which provides abundant edge defects. Edge defects are favorable to the capacitance of a supercapacitor [28]. In order to certify the existence of edge defects on vertically oriented graphene, VOG-10 were further characterized by Raman spectroscopy and electron energy loss spectroscopy (EELS). The Raman spectrum provides useful information about the defects, in-plane vibration of sp2 carbon atoms, as well as the stacking order. Fig. 2h shows the Raman spectrum of VOG-10, in which, in addition to the typical D and G peaks, a symmetric single 2D peak at $\sim$2700 cm^{-1} is observed, which stems from the second order of the zone-boundary phonons and is closely related to the layer number of graphene [29]. The D peak is related to the disorders and defects of graphene [30], and the intensity of the D peak relative to the G peak (I_D/I_G) reflects the abundance of defects in graphene. Compared with normal CVD graphene [31], the Raman spectrum of VOG-10 exhibits a much stronger defect peak, which consists with the edge defects of few-layer graphene as shown in the TEM image of Fig. 2g. There is a split peak labeled G at 1621 cm^{-1}, which is due to in-plane vibrations along the vertically grown axis. The full-width at half-height maximum of 2D bond is 50 cm^{-1}, and the intensity ratio of G/2D

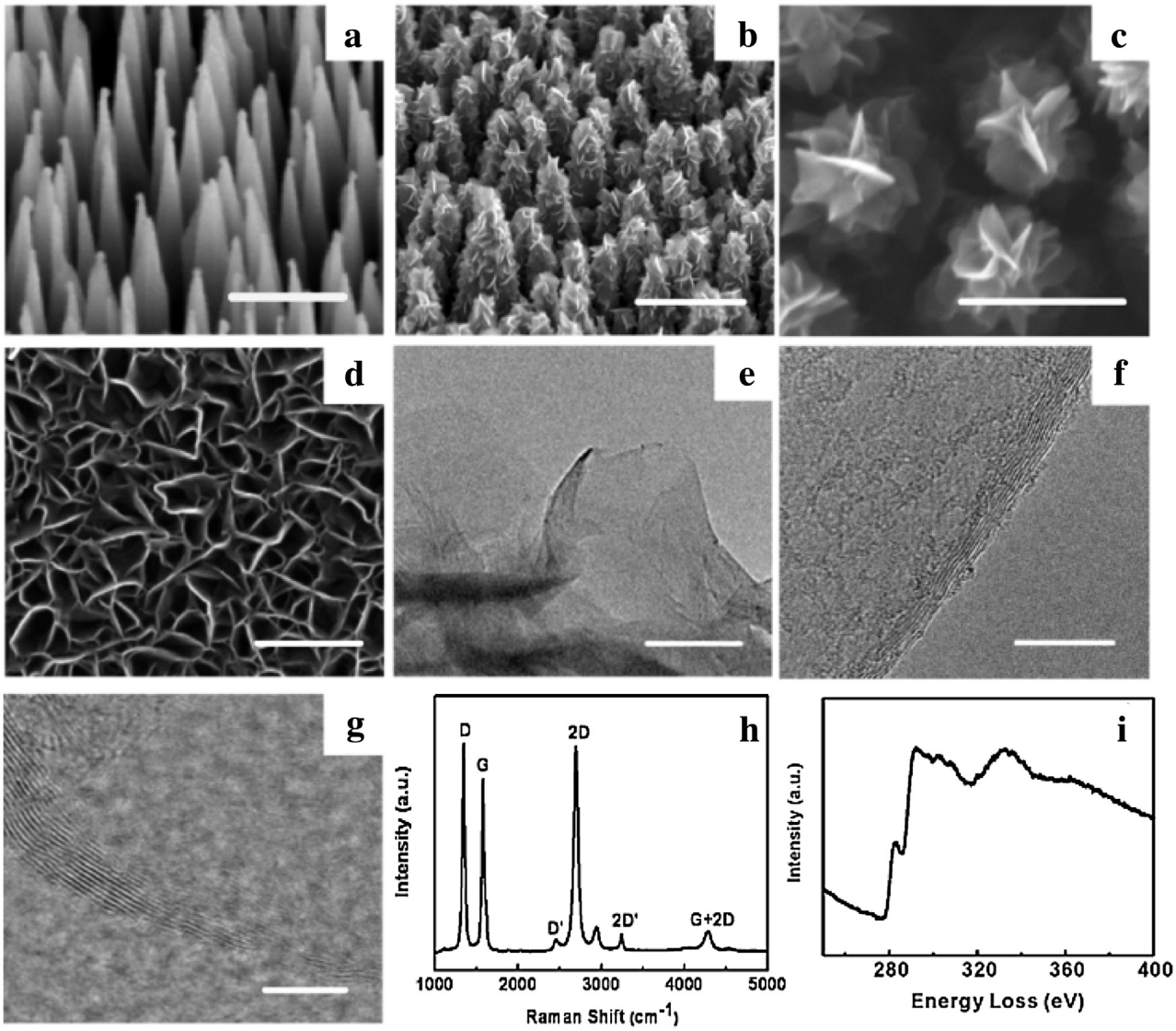

Fig. 2. (a) SEM image of silicon nanocone arrays. (b) and (c) are side-view and top-view SEM images of vertically oriented graphene grown on Si nanocone arrays, respectively. (d) Top view SEM image of vertically oriented few-layer graphene grown on flat silicon wafer. (e) TEM image of CVD graphene with growth time of 10 min. (f) and (g) are high-resolution TEM images of graphene nanosheet and edge, respectively. Scale bar is 1 μm in a and b, and 400 nm in c and d, 20 nm in e, 10 nm in f, 5 nm in g. (h) Raman spectrum of vertically oriented graphene with 10 min of growth time. (i) The electron energy loss spectrum of vertically oriented graphene.

is about 0.85. Thus the number of layers for VOG-10 is estimated to be between 8 and 15. Fig. 2i is a typical EELS spectrum of the as grown VOG-10 that reveals the stoichiometric information of our few-layer graphene. The two main features of a graphene EELS spectrum in the carbon K-edge region are that a peak located at 285 eV that corresponds to transitions from the 1 s to the π^* states (1s-π^*) and a peak centered at 291 eV that corresponds to transitions from the σ^* states [32]. Most of the carbon atoms are in a highly oriented arrangement, and no trace of impurities (chemical functional group) is observed in the EELS spectrum.

3.2. Evaluation of the performance of 3D EDLCs

The electrochemical performance of supercapacitors was analyzed using cyclic voltammetry (CV), electrochemical impedance spectra (EIS) and a life test with a two-electrode setup at room temperature. CV tests were performed at scan rates ranging from 50 to 10,000 mVs^{-1} with a potential ranging from 0 to 1 V. Fig. 3a shows the CV curves of VOG-10 at scan rates of 100–10,000 mVs^{-1}. All the CV curves in Fig. 3a show nearly symmetrical rectangular shapes, indicating an ideal capacitive behavior and a good rate capability. The areal capacitance was calculated according to the CV curves [33]. The specific capacitances were obtained depending on different voltage scan rates, which are listed in Fig. 3b. At a scan rate of 100 mVs^{-1}, the area specific capacitance of VOG-10 EDLC electrode reaches 667.2 $\mu F\,cm^{-2}$, which is several times larger than previously reported data (120 μFcm^{-2} [34] and 238 $\mu F\,cm^{-2}$ [35]). At scan rate of 10,000 mVs^{-1}, the capacitance was maintained at 400 $\mu F\,cm^{-2}$, which shows an ultrahigh rate capability. EIS analysis was used to check the charge transport of VOGs as shown as in Fig. 3c. The measurements were performed at open circuit voltage (OCV) by applying a sinusoidal signal of 10 mV amplitude at frequencies ranging from 100 kHz to 1 Hz. The plot features a vertical curve, indicating a nearly ideal capacitive behavior of the supercapacitor. In a higher frequency region (Fig. S2 in Supplemental information), the semicircle cannot be observed for samples with Ni film deposited as a conducting layer. This reveals the negligible charge transfer resistance, which further implies the advantages of the 3D design that guarantees ion and charge transfer as well as good electric contact with the current collector. The inset of Fig. 3c

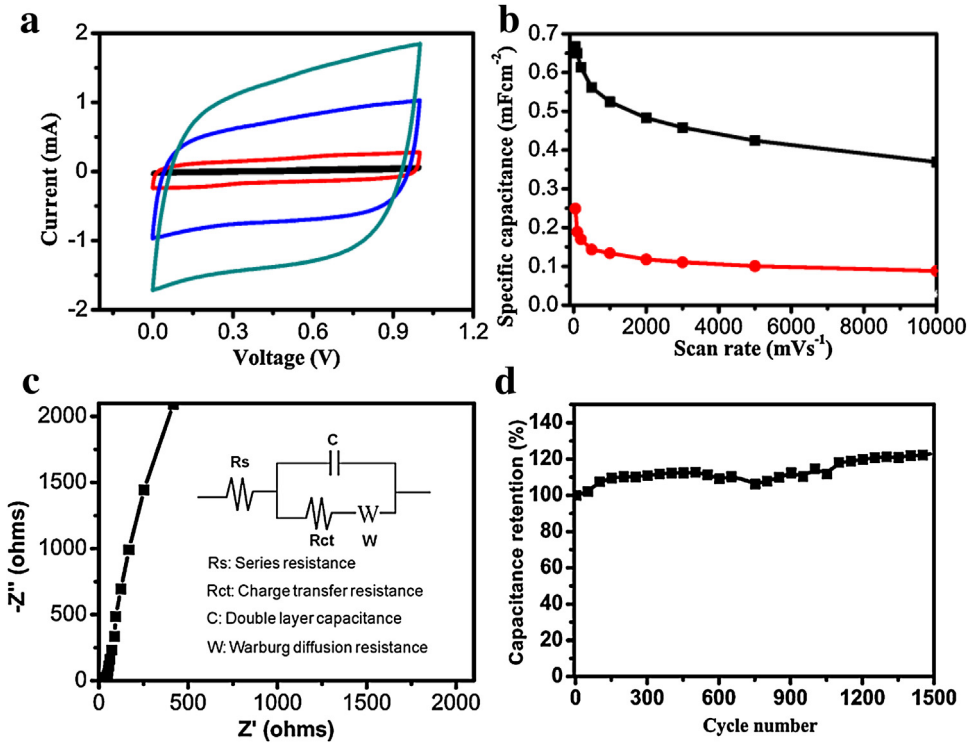

Fig. 3. Electrochemical performance of the VOG-10 EDLC in PVA-KOH gelled electrolyte. (a) The CV curves of the device with scan rates of 100 mVs^{-1} (black curve), 1000 mVs^{-1} (red curve), 5000 mVs^{-1} (blue curve) and 10,000 mVs^{-1} (green curve). (b) Comparison of the capacitance of EDLCs based on VOG-10 electrode based on flat substrate (red curve with filled circles) and VOG-10 on 3D silicon nanocone substrate (black curve with filled squares) at different voltage scan rates. (c) Nyquist plots of VOG-10 device obtained at 0–1 V open circuit potential over frequencies ranging from 100 kHz to 1 Hz; inset is the equivalent circuit for the VOG-10 EDLC. (d) Cycle life of VOG-10 EDLC tested at scan rate of 1000 mVs^{-1} for 1500 cycles. (For interpretation of the references to colour in this figure legend, the reader is referred to the web version of this article.)

shows the proposed equivalent circuit. In the Nyquist plot, from the point intersecting with the real axis in the high frequency area, the internal resistance can be read as 34 Ω, which corresponds to Rs in the circuit. The charge transfer resistance is calculated to be 3×10^{-3} Ω, while the Warburg diffusion resistance is 1×10^{-4} Ω. A simulation of equivalent circuit calculation indicates the excellent ion transport in the device [36,37]. Cycle life of the device is further tested under 1000 mVs^{-1} for 1500 cycles (Fig. 3d). No attenuation was observed, and interestingly, there is no any decay in capacitance after 1500 cycles of charging/discharging, suggesting extremely stable capacitive behavior. Furthermore, cyclic stability measurement by using consecutive CV scans in KOH aqueous solution show that there is also no any decay in capacitance even after 5000 CV scanning cycles which also demonstrates the as-prepared graphene supercapacitor possesses superior cyclic stability (see Fig. S3 in Supplemental information). Moreover, electrodes with 2D planar Si chips as current collector substrates with 200 nm Ni film and graphene of 10 min CVD growth-time were fabricated as a control sample in order to illustrate the advantages of the 3D structure. A schematic of the EDLC configuration based on 2D planar electrodes is shown in Fig. S4 (Supplemental information). Compared with the schematic of 3D electrode in Fig. 1a, the 2D planar electrode possesses less surface area and exhibits enhanced areal capacitance. A comparison of specific capacitances of EDLCs based on 2D planar electrodes with 3D electrodes is shown in Fig. 3b. Note that the areal capacitance of 3D EDLC is about 4 times larger than that of a flat EDLC. This is evidence of the enhancement of the 3D electrode design on the capacitance of EDLCs.

The galvanostatic charge/discharge curves of the VOG-10 EDLC with a current density varying from 0.1 $mAcm^{-2}$ to 1 $mAcm^{-2}$ is plot in Fig. S5 (Supplemental information). A linear dependence of the discharge curves and time indicate a non-faradic characteristic in the VOG-10 EDLC. The highly linear curves also demonstrated an outstanding charge/discharge property. And the IR drop that indicating a voltage lose when tune the charge current to discharge current can be neglect in VOG-10 EDLC, which suggesting a slight influence equivalent series resistance (ESR).

3.3. *Effect of graphene growth time on performance of EDLCs*

To investigate the relationship between the quality of graphene and the performance of supercapacitors, more samples of vertically oriented graphene on silicon nanocone were synthesized with various growth times. Vertically oriented graphene based electrodes were dubbed VOG-5, VOG-20 and VOG-30, corresponding to their CVD growth time (5 min, 20 min and 30 min). The morphology variation of as grown VOG-5, VOG-10, VOG-20 and VOG-30 is shown in Fig. 4a–d. The specific surface area and porosity analysis of these 3D electrodes is critical to the performances of EDLCs. Generally, specific surface area and porosity can be calculated from the experimental data of Brunauer–Emmer–Teller (BET) test, but unfortunately the overall weight of graphene nanosheets is insufficient to get any reliable surface area data. The porosity of the 3D electrodes ranges from 60 to 30% for VOG-5, VOG-10, VOG-20 and VOG-30. Four supercapacitors based on 3D electrodes with VOG-5, VOG-10, VOG-20 and VOG-30 were prepared and tested using CV tests to compare their capacitance and capacitance retention with a change of scan rates. All the CV curves are shown in Fig. S6 (Supplemental information). Based on these results, Fig. 4f gives the areal capacitances of devices based on VOG-5, VOG-10, VOG-20 and VOG-30 electrodes at different scan rates. The sample of VOG-10 has largest capacitance, as shown in Fig. 4a. Meanwhile, the VOG-10 EDLC also exhibits the best rate performance with capacitance retention of 63.6%, when the scan rate changes from 50 mVs^{-1} to 5000 mVs^{-1}. The capacitance and rate performance of VOG-20 and VOG-5 are slightly inferior to those of VOG-10. From the Nyquist

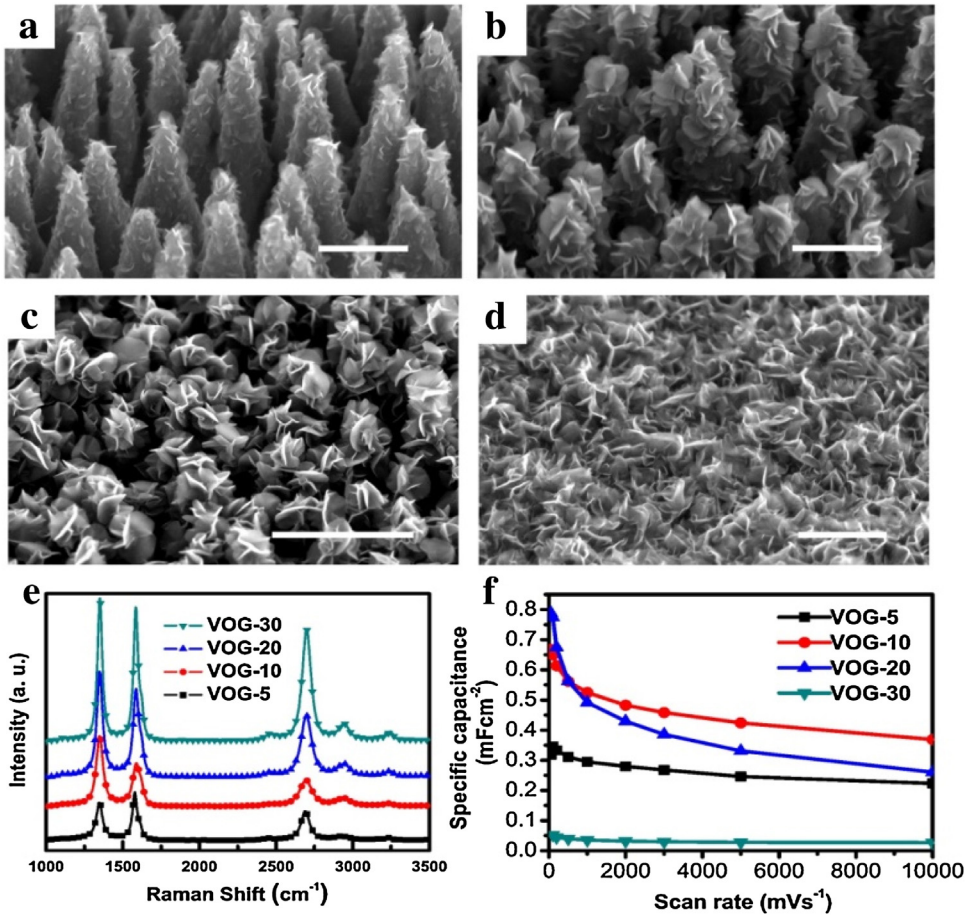

Fig. 4. (a)–(d) SEM images with 45° tilt of VOG-5, VOG-10, VOG-20 and VOG-30 electrodes on 3D silicon nanocone substrate. Scale bars are 500 nm in a–c, and 1 μm in d. (e) Raman spectra of vertically oriented graphene with different growth times. (f) Comparison of the capacitance of EDLCs based on VOG-5, VOG-10, VOG-20 and VOG-30 3D electrodes.

plots in Fig. S7a (Supplemental information), it is observed that there is no obvious difference in ESR between VOG-10, VOG-20 and VOG-30. On the contrary, VOG-5 shows the largest ESR. In the low frequency part, however, the VOG-10 tends to exhibit the most vertical line, which implies the best capacitor behavior. This is consisted with their rate performance behavior. In order to explain this discrepancy, we analyzed the vertically oriented graphene-based electrodes with SEM images. Fig. S4a–d shows the evolution of graphene with growth-time varied from 5 min to 30 min. It can be observed that with growth-time increasing, the size and density of graphene sheets changes obviously. At the beginning of the growth, the sheets of vertically oriented graphene were rather small with a big interval from silicon nanocone substrate. Then the graphene sheets grow while the spaces among nanocones shrink. At growth duration of 10 min, flourishing graphene nanosheet arrays with proper spacing between clusters were formed. After 30 min, as-grown vertically oriented graphene submerged the silicon nanocones completely, and both the spaces and the feature of cones disappeared (Fig. 4f). So the largest ESR of VOG-5 is because the graphene sheets have not covered the electrode completely after just growing 5 min. In contrast, VOG-30 has too few channels for ions to transfer and absorb, so the morphology inhibits its electrochemical performance.

Raman spectra of the four samples were also collected as shown in Fig. 4g. Characteristic peaks of each graphene samples can be clearly observed (Fig. 4g). As is well known, the ratio of I_D to I_G indicates the defects of graphene, while I_{2D} to I_G indicates the number of layers [38,39]. According to intensity ratio calculation results listed in Fig. S7b (Supplemental information), the value of I_{2D}/I_G gradually increases as the growing time increases, which means the graphene becomes multilayer structure as growing time progresses, consistent with the SEM results in Fig. 4a–d. Besides, VOG-10 has the largest I_{2D}/I_G value, which reveals the VOG-10 has most edge defects. Generally, the defects possess higher activity level and thus give rise to capacitance [40]. It is noted that the defects of sample VOG-30 are more abundant than those of VOG-5 (Fig. S7b, Supplemental information), while the capacitance is far lower than VOG-5 (shown in Fig. 4f). We propose that excessive growth time leads to re-stacking of graphene after 20 min and results in the graphene on different micro-cones overlapping, which reduces the active surface of graphene and results in a lower capacitance than VOG-5.

We attribute the enhancement of capacitance and rate capability of our EDLCs to the special structure of 3D electrodes. The design of these 3D electrodes takes advantage of Si nanocones and CVD vertically oriented graphene. First, the micro-structured silicon cone arrays enhance the surface area by a factor of ca. 6, which improves the amount of active materials loaded per unit area on the Si chip and hence results in a larger capacitance per unit area. Besides, the vertically oriented graphene can effectively avoid the restacking of the graphene layers, which makes larger active surfaces available to electrolytes and thus further promotes the double-layer capacitances of graphene. Second, the graphene that is directly deposited on the current collectors by the CVD process possesses outstanding contact, which reduces the contact resistance between the graphene and the current collector and enhances the

adhesion of graphene with current collectors. Thus, the rate capability and the cyclic stability are both improved. Furthermore, the open structure among silicon micro-cones and the vertical orientation, together, benefit ion diffusion during the charge/discharge process and also result in the improved rate capability. All these factors endow the VOG-10 EDLC with an area specific capacitance of 667.2 $\mu F\,cm^{-2}$, which is about four times that in supercapacitors with vertically aligned graphene on the 2D planar electrode. This unique design of electrodes with 3D nanostructured current collector and vertically oriented graphene promotes the main characteristics of supercapacitors: energy density (i.e. capacitance) and power density (i.e. rate capability). In short, the strategy of 3D structure of CVD graphene-based electrodes is a valuable effort to improve the capacitance of EDLCs without sacrificing their power density and cycle life.

4. Conclusions

We have designed a new type of 3D graphene-based supercapacitor, which possesses extremely high areal capacitance and rate capability, by combining vertically oriented graphene with a 3D nanocone configuration. Electrodes with high density of edge defects of graphene were obtained by taking advantage of the silicon nanocone structure and the CVD growth method of graphene. The electrode with 10 min of CVD growth of graphene endows EDLCs with a specific capacitance of 667.2 $\mu F\,cm^{-2}$, which is several times larger than previously reported data. We propose that the origins for the high electrochemical performance be ascribed to large surface area, high edge defects density and superior ion accessibility. Extremely high specific capacitance, excellent rating capability and stable capacitance retention performance were acquired due to the unique structure of the 3D Si nanocone arrays and vertically oriented graphene. This work provides a new strategy to improve capacitance with microfabrication technologies and CVD deposition, which promote the progress and commercialization of supercapacitors.

Acknowledgements

The authors acknowledge This work is supported by the Ministry of Science and Technology of China (2016YFA0200803, 2016YFA0200802, 2016YFA0200402, 2016YFB0100500), the National Natural Science Foundation of China (Grant Nos. 91323304, 11674387, 61390503, 11574369, 91436102), and the Strategic Priority Research Program of the Chinese Academy of Sciences (Grant No. XDB07020200).

Appendix A. Supplementary data

Supplementary data associated with this article can be found, in the online version, at http://dx.doi.org/10.1016/j.apsusc.2017.01.312.

References

[1] J.R. Miller, R.A. Outlaw, B.C. Holloway, Graphene double-layer capacitor with ac line-filtering performance, Science 329 (2010) 1637–1639.
[2] P. Simon, Y. Gogotsi, Materials for electrochemical capacitors, Nat. Mater. 7 (2008) 845–854.
[3] L.L. Zhang, X.S. Zhao, Carbon-based materials as supercapacitor electrodes, Chem. Soc. Rev. 38 (2009) 2520–2531.
[4] G. Wang, L. Zhang, J. Zhang, A review of electrode materials for electrochemical supercapacitors, Chem. Soc. Rev. 41 (2012) 797–828.
[5] Y. Zhu, S. Murali, M.D. Stoller, K.J. Ganesh, W.W. Cai, P.J. Ferreira, A. Pirkle, R.M. Wallace, K.A. Cychosz, M. Thommes, D. Su, E.A. Stach, R.S. Ruoff, Carbon-based supercapacitors produced by activation of graphene, Science 332 (2011) 1537–1541.
[6] Z.S. Wu, K. Parvez, X. Feng, K. Mullen, Graphene-based in-plane micro-supercapacitors with high power and energy densities, Nat. Commun. 4 (2013) 2487–2493.
[7] J. Chmiola, G. Yushin, Y. Gogotsi, C. Portet, P. Simon, P.L. Taberna, Anomalous increase in carbon capacitance at pore sizes less than 1 nanometer, Science 313 (2006) 1760–1763.
[8] M.F. El-Kady, V. Strong, S. Dubin, R.B. Kaner, Laser scribing of high-performance and flexible graphene-based electrochemical capacitors, Science 335 (2012) 1326–1330.
[9] H.X. Ji, X. Zhao, Z.H. Qiao, J. Jung, Y.W. Zhu, Y.L. Lu, L.L. Zhang, A.H. MacDanald, R.S. Ruoff, Capacitance of carbon-based electrical double-layer capacitors, Nat. Commun. 5 (2014) 3317–3323.
[10] A.K. Geim, K.S. Novoselov, The rise of graphene, Nat. Mater. 6 (2007) 183–191.
[11] X.W. Yang, C. Cheng, Y.F. Wang, L. Qiu, D. Li, Liquid-mediated dense integration of graphene materials for compact capacitive energy storage, Science 341 (2013) 534–537.
[12] G.F. Ren, X. Pan, S. Bayne, Z.Y. Fan, Kilohertz ultrafast electrochemical supercapacitors based on perpendicularly-oriented graphene grown inside of nickel foam, Carbon 71 (2014) 94–101.
[13] Z. Bo, W.G. Zhu, W. Ma, Z.H. Wen, X.R. Shuai, J.H. Chen, J.H. Yan, Z.H. Wang, K.F. Cen, Vertically oriented graphene bridging active-layer/current-collector interface for ultrahigh rate supercapacitors, Adv. Mater. 25 (2013) 5799–5806.
[14] W.X. Song, X.J. Ji, W.T. Deng, Q.Y. Chen, C. Shen, C.E. Banks, Graphene ultracapacitors: structural impacts, Phys. Chem. Chem. Phys. 15 (2013) 4799–4803.
[15] Y.N. Meng, K. Wang, Y.J. Zhang, Z.X. Wei, Hierarchical porous graphene/polyaniline composite film with superior rate performance for flexible supercapacitors, Adv. Mater. 25 (2013) 6985–6990.
[16] Y.H. Yoon, K. Lee, C. Baik, H.J. Yoo, M. Min, Y.H. Park, S.M. Lee, H. Lee, Anti-solvent derived non-stacked reduced graphene oxide for high performance supercapacitors, Adv. Mater. 25 (2013) 4437–4444.
[17] H. Jiang, P.S. Lee, C.Z. Li, 3D carbon based nanostructures for advanced supercapacitors, Energy Environ. Sci. 6 (2013) 41–53.
[18] J.J. Yoo, K. Balakrishnan, J.S. Huang, V. Menuier, B.G. Sumpter, A. Srivastava, M. Conway, A.L.M. Reddy, J. Yu, R. Vajtai, P.M. Ajayan, Ultrathin planar graphene supercapacitors, Nano Lett. 11 (2011) 1423–1427.
[19] S.B. Tian, L. Li, W.N. Sun, X.X. Xia, D. Han, J.J. Li, C.Z. Gu, Robust adhesion of flower-like few-layer graphene nanoclusters, Sci. Rep. 2 (2012) 511–517.
[20] X.S. Li, W.W. Cai, J.H. An, S. Kim, J. Nah, D.X. Yang, R. Piner, A. Velamakanni, I. Jung, E. Tutuc, S.K. Banerjee, L. Colombo, R.S. Ruoff, Large-area synthesis of high-quality and uniform graphene films on copper foils, Science 324 (2009) 1312–1314.
[21] S.S. Chen, W.W. Cai, R.D. Piner, J.W. Suk, Y.P. Wu, Y.J. Ren, J.Y. Kang, R.S. Ruoff, Synthesis and characterization of large-area graphene and graphite films on commercial Cu–Ni alloy foils, Nano Lett. 11 (2011) 3519–3525.
[22] N.S. Choi, Z.H. Chen, S.A. Freunberger, X.L. Ji, Y.K. Sun, K. Amine, G. Yushin, L.F. Nazar, J. Cho, P.G. Bruce, Challenges facing lithium batteries and electrical double-layer capacitors, Angew. Chem. Int. Ed. 51 (2012) 9994–10024.
[23] M. Beidaghi, Y. Gogotsi, Capacitive energy storage in micro-scale devices: recent advances in design and fabrication of micro-supercapacitors, Energy Environ. Sci. 7 (2014) 867–884.
[24] A.S. Arico, P. Bruce, B. Scrosati, J.M. Tarascon, W. van Schalkwijk, Nanostructured materials for advanced energy conversion and storage devices, Nat. Mater. 4 (2005) 366–377.
[25] J.L. Qi, X. Wang, J.H. Lin, F. Zhang, J.C. Feng, W.D. Fei, Vertically oriented few-layer graphene-nanocup hybrid structured electrodes for high-performance supercapacitors, J. Mater. Chem. A 3 (2015) 12396–12403.
[26] H.C. Yang, J.Y. Yang, Z. Bo, S. Zhang, J.H. Yan, K.F. Cen, Edge effects in vertically-oriented graphene based electric double-layer capacitors, J. Power Sources 324 (2016) 309–316.
[27] L. Li, W.N. Sun, S.B. Tian, X.X. Xia, J.J. Li, C.Z. Gu, Floral-clustered few-layer graphene nanosheet array as high performance field emitter, Nanoscale 4 (2012) 6383–6388.
[28] J. Wu, W. Pisula, K. Mullen, Graphenes as potential material for electronics, Chem. Rev. 107 (2007) 718–747.
[29] M.S. Dresselhaus, A. Jorio, M. Hofmann, G. Dresselhaus, R. Saito, Perspectives on carbon nanotubes and graphene Raman spectroscopy, Nano Lett. 10 (2010) 751–758.
[30] Y. Wang, D.C. Alsmeyer, R.L. McCreery, Raman spectroscopy of carbon materials: structural basis of observed spectra, Chem. Mater. 2 (1990) 557–563.
[31] L.M. Malard, M.A. Pimenta, G. Dresselhaus, M.S. Dresselhaus, Raman spectroscopy in graphene, Phys. Rep. 473 (2009) 51–87.
[32] L.S. Panchakarla, K.S. Subrahmanyam, S.K. Saha, A. Govindaraj, H.R. Krishnamurthy, U.V. Waghmare, C.N.R. Rao, Synthesis structure, and properties of boron-and nitrogen-doped graphene, Adv. Mater. 21 (2009) 4726–4730.
[33] M.D. Stoller, R.S. Ruoff, Best practice methods for determining an electrode material's performance for ultracapacitors, Energy Environ. Sci. 3 (2010) 1294–1301.
[34] M.Z. Cai, R.A. Outlaw, S.M. Butler, J.R. Miller, A high density of vertically-oriented graphenes for use in electric double layer capacitors, Carbon 50 (2012) 5481–5488.
[35] K.X. Sheng, Y.Q. Sun, C. Li, W.J. Yuan, G.Q. Shi, Ultrahigh-rate supercapacitors based on eletrochemically reduced graphene oxide for ac line-filtering, Sci. Rep. 2 (2012) 247.

[36] B.G. Choi, J. Hong, W.H. Hong, P.T. Hammond, H. Park, Facilitated ion transport in all-solid-state flexible supercapacitors, ACS Nano 5 (2011) 7205–7213.
[37] E. Barsoukov, J.R. Macdonald, Impedance Spectroscopy: Theory, Experiment, and Applications, 2nd ed., John Wiley & Sons, Inc., Hoboken, 2005.
[38] J.R. Miller, R.A. Outlaw, B.C. Holloway, Graphene electric double layer capacitor with ultra-high-power performance, Electrochim. Acta 56 (2011) 10443–10449.
[39] A.C. Ferrar, J.C. Meyer, V. Scardaci, C. Casiraghi, M. Lazzeri, F. Mauri, S. Piscanec, D. Jiang, K.S. Novoselov, S. Roth, A.K. Geim, Raman spectrum of graphene and graphene layers, Phys. Rev. Lett. 97 (2006) 187401–187404.
[40] D.W. Boukhvalov, M.I. Katsnelson, Chemical functionalization of graphene with defects, Nano Lett. 8 (2008) 4373–4379.